

# Response to Reviewers

## Comment on acp-2022-292

### RC2 Anonymous Referee #2

Review of “Seasonal characteristics of atmospheric formaldehyde (HCHO) in a coastal city of southeast China: Formation mechanism and photochemical effects,” Liu et al., ACP (2022)

#### Summary

This manuscript describes a set of ground-based observations of atmospheric composition at a coastal urban site in China. The primary analysis focus is formaldehyde (HCHO). Measurements are fed into a PMF model and a photochemical box model to estimate the sources of HCHO and the contributions of HCHO to radical chemistry and ozone production.

The reviewer has substantial concerns regarding the quality of HCHO observations, the interpretation of the PMF and box model results, and the general presentation of data and analysis. Many superfluous details are provided in the text. Text is highly descriptive without drawing out any obvious novel/new conclusions. This is a potentially useful contribution that hopefully will benefit from a hard critique. I recommend rejection with encouragement to resubmit.

**Response:** Thanks for your feedback on the whole manuscript and valuable comments on some details. The detailed introduction of HCHO observations was added to our manuscript, and the related issues of PMF and box model have also been explained and resolved. We have tried our best to improve the quality of this manuscript. Many analyses have been improved to be complete and easy to understand accordingly.

#### General Comments

Regarding the HCHO analyzer described in Sect. 2.1: The reviewer was not able to locate any information about this analyzer on the internet, and there is no citation of literature regarding the design or performance of this instrument. The stated performance is 1 Hz, 50 pptv detection limit, 5% accuracy. This exceeds, by far, similar Hantzsch-based instruments. For example, Glowania et al. (2021) report a 90-second time response, 300 pptv detection limit, and 8.6% accuracy (<https://doi.org/10.5194/amt-14-4239-2021>). Given that HCHO is central to this paper, additional documentation regarding calibration procedures and determination of potential artifacts is warranted.

**Response:** Thanks for your suggestion. The reaction chamber system of our HCHO analyzer has optimizations compared to theirs (Glowania et al. 2021). The HCHO analyzer was customized by Hangzhou Focused Photonics Inc., of which the patent was announced in December 2020 (Wang et al., 2020) and there are currently no published researches to cite. Formaldehyde standard solution can react with Hantzsch reagent at room temperature with a slow reaction speed. In this study, stainless steel tube for heating efficiency and ceramic fiber board thermal insulation layer for thermal insulation efficiency were used to control the reaction temperature of the mixed solution in the reaction chamber to shorten the reaction time, which reduced the time required for thermal equilibrium significantly, achieving a signal acquisition frequency of 1 per second.

After completing the multi-point calibration, zero gas tests for more than 1 hour were carried out, then the standard deviations of 60 sets of gas concentration data were obtained, and the detection limit was 3 times the standard deviation. Table S1 shows the detection limit results in our study.

**Table S1. The detection limit.**

Time	HCHO (ppbv)	Time	HCHO (ppbv)
2021-05-14 01:06:58	-0.168	2021-05-14 01:07:28	-0.157
2021-05-14 01:06:59	-0.167	2021-05-14 01:07:29	-0.157
2021-05-14 01:07:00	-0.166	2021-05-14 01:07:30	-0.157
2021-05-14 01:07:01	-0.165	2021-05-14 01:07:31	-0.156
2021-05-14 01:07:02	-0.164	2021-05-14 01:07:32	-0.156
2021-05-14 01:07:03	-0.163	2021-05-14 01:07:33	-0.156
2021-05-14 01:07:04	-0.162	2021-05-14 01:07:34	-0.155
2021-05-14 01:07:05	-0.161	2021-05-14 01:07:35	-0.155
2021-05-14 01:07:06	-0.161	2021-05-14 01:07:36	-0.154
2021-05-14 01:07:07	-0.161	2021-05-14 01:07:37	-0.154
2021-05-14 01:07:08	-0.161	2021-05-14 01:07:38	-0.154
2021-05-14 01:07:09	-0.16	2021-05-14 01:07:39	-0.153
2021-05-14 01:07:10	-0.16	2021-05-14 01:07:40	-0.153
2021-05-14 01:07:11	-0.159	2021-05-14 01:07:41	-0.153
2021-05-14 01:07:12	-0.159	2021-05-14 01:07:42	-0.153
2021-05-14 01:07:13	-0.158	2021-05-14 01:07:43	-0.152
2021-05-14 01:07:14	-0.158	2021-05-14 01:07:44	-0.152
2021-05-14 01:07:15	-0.158	2021-05-14 01:07:45	-0.151
2021-05-14 01:07:16	-0.158	2021-05-14 01:07:46	-0.151
2021-05-14 01:07:17	-0.158	2021-05-14 01:07:47	-0.15
2021-05-14 01:07:18	-0.158	2021-05-14 01:07:48	-0.15
2021-05-14 01:07:19	-0.158	2021-05-14 01:07:49	-0.149
2021-05-14 01:07:20	-0.158	2021-05-14 01:07:50	-0.149
2021-05-14 01:07:21	-0.158	2021-05-14 01:07:51	-0.148
2021-05-14 01:07:22	-0.158	2021-05-14 01:07:52	-0.147

2021-05-14 01:07:23	-0.158	2021-05-14 01:07:53	-0.146
2021-05-14 01:07:24	-0.158	2021-05-14 01:07:54	-0.146
2021-05-14 01:07:25	-0.158	2021-05-14 01:07:55	-0.145
2021-05-14 01:07:26	-0.157	2021-05-14 01:07:56	-0.144
2021-05-14 01:07:27	-0.157	2021-05-14 01:07:57	-0.144
Standard deviation		0.0056	
Detection limit (ppbv)		0.017	

After completing the multi-point calibration, three different concentrations of standard solutions were measured for 30 minutes under the liquid measurement mode, and the zero-gas mode was used at 10-minute intervals. Take 300 groups of data in each liquid measurement mode of the same concentration standard solution, and calculate the accuracy and repetition rate of three different concentration standard solutions respectively. Table S2 shows the accuracy and repetition rate of three different concentrations in our study.

**Table S2. The accuracy and repetition rate.**

Standard solution (ppbv / $\mu\text{g}\cdot\text{L}^{-1}$ )	Measured ( $\mu\text{g}\cdot\text{L}^{-1}$ )	Accuracy (%)	Repetition rate (%)
10 / 29.892	29.683	-0.70	1.00
25 / 74.709	74.811	0.14	0.06
40 / 119.499	123.444	3.30	0.64

The detailed description of the HCHO analyzer was added in the manuscript and the Supplementary, and the relevant revised content in the manuscript is as follows:

“HCHO analyzer (FMS-100, Focused Photonics Inc., Hangzhou, China) was used to monitor the HCHO mixing ratios with a temporal resolution of 1 s, which collected gaseous HCHO at a flow rate of  $1 \text{ L}\cdot\text{min}^{-1}$  by an  $\text{H}_2\text{SO}_4$  stripping solution and quantified HCHO mixing ratios through detection by fluorescence at  $\lambda=510 \text{ nm}$  (Hu et al., 2022; Glowania et al., 2021). The HCHO liquid solution quantification is based on the Hantzsch reaction, but the reaction speed is slow at room temperature (Glowania et al., 2021). In our study, stainless steel tube for heating efficiency and ceramic fiber board thermal insulation layer for thermal insulation efficiency were used to control the reaction temperature of the mixed solution in the reaction chamber to shorten the reaction time, which reduced the time required for thermal equilibrium significantly, achieving a high signal acquisition frequency. The different dilutions of the HCHO standard solution and a blank were used to make a multi-point calibration every week for obtaining a curve with  $R^2 \geq 0.999$ . In these conditions, the limit of detection was 50 pptv and the uncertainty was  $\leq 5\%$  in this study. The detailed detection limit, accuracy, and repetition rate testing were shown in Table S1 and Table S2.”

Regarding interpretation of a highly-constrained model: Throughout the text, attention is given to the difference between HCHO production and loss rates (described as “net production rate” on L181). The model, however, is forced to measured HCHO. How well does the model predict HCHO if this constraint is turned off? If the model performs poorly, this calls into question the utility of the “net production rate” since the HCHO concentration does not match what would be predicted based on the modeled gross production rate.

**Response:** Thanks for your suggestion. We turned off the observed HCHO values to discuss the model predicting HCHO, and Figure S1 shows the simulated and observed HCHO at the study site. In general, the model overestimated HCHO concentration. According to previous studies, the inconsistency between simulated and observed HCHO could be caused by the uncertainties in the treatment of dry deposition, faster vertical transport, uptake of HCHO, atmospheric diffusion/dilution meteorological conditions, and fresh emission of precursor VOCs (Li et al., 2014; Zhang et al., 2021). The index of agreement (IOA) (Zhang et al., 2021), which was calculated by the differences between the modeled HCHO concentrations and observed concentrations, is used to judge the rationality of the model results (detailed introduction of IOA was shown in the first question of (Professor Ye Referee #1)).

The IOA range is 0-1, and the higher the IOA value is, the better agreement between modeled and observed values is. In many studies, IOA ranges from 0.68 to 0.89 (Wang et al., 2018), and the modeled results are reasonable. The IOAs in spring and autumn in our research are 0.83 and 0.80, respectively. Although there is a certain discrepancy, the model could generally reflect the atmospheric chemical processes, and these results still provide valuable information on secondary formation of HCHO at our study site.

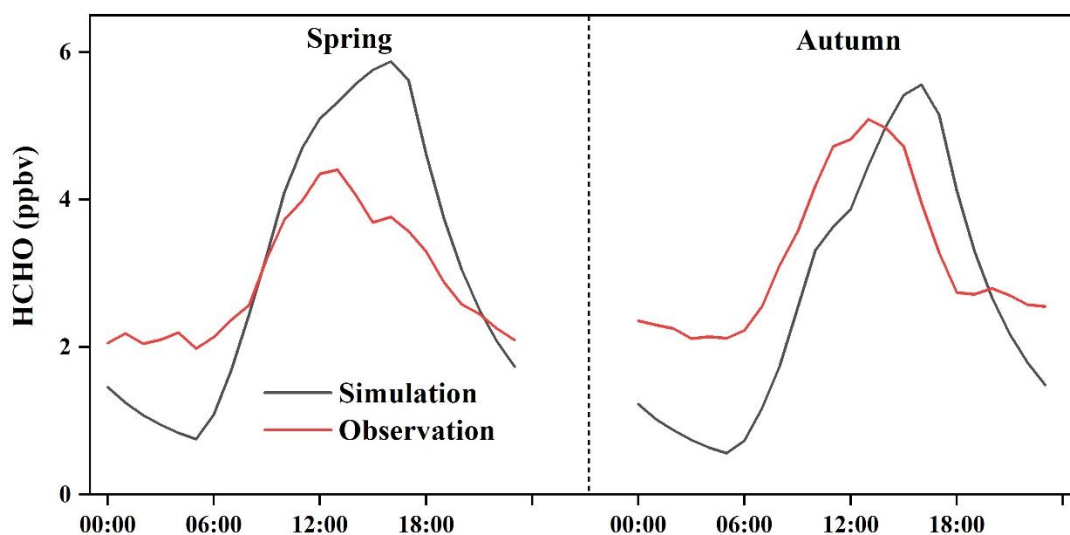


**Figure S1. The simulated and observed HCHO at the study site.**

PMF analysis: Several questions here.

1. Why are other species not included in PMF (CO, NO<sub>x</sub>, PAN)? In particular, CO should be a clear marker of vehicle exhaust.

**Response:** Thanks for your suggestion. Our idea is to analyze the source distribution of VOCs, and then determine the contribution of different sources to HCHO. Hence, we chose HCHO, 17 NMHCs, 1,2-dichloroethane, and O<sub>3</sub> to put into the PMF model together, and these species were selected because most of them are typical tracers of specific sources and have relatively high concentrations. Among them, O<sub>3</sub> is used as a surrogate for photochemical processes to determine the secondary fraction of HCHO, and the NMHCs of 3-methylpentane, iso-pentane, the light hydrocarbons of n/iso-pentane and n/iso-butane also are good indicators of vehicle exhaust. Hence, the species of CO, NO<sub>x</sub>, and PAN are not included in PMF. The model validation in our study indicated PMF reasonably identified the contributions of primary and secondary sources of HCHO, and the detailed model validation information shows in the first question of Professor Ye (Referee #1). In previous studies, the researchers of Ling et al. (2017) and Zeng et al. (2019) adopted the same method to analyze HCHO based on PMF. The detailed introduction is also added to the manuscript in Section 2.2, as follows:

“In our study, we chose HCHO, 17 Non-Methane Hydrocarbons (NMHCs), 1,2-dichloroethane, and O<sub>3</sub> to put into the PMF model, which are typical tracers of specific sources and have relatively high concentrations. Among them, O<sub>3</sub> is used as a surrogate for photochemical processes to determine the secondary fraction of HCHO (Ling et al., 2017; Zeng et al., 2019).”

2. Are the authors really suggesting that the HCHO associated with isoprene is directly emitted by the ecosystem? Is there any literature evidence of that? It seems more likely that this HCHO was produced by isoprene enroute to the site. Possibly without significant ozone production (e.g. from a nearby forest).

**Response:** We are sorry for the confusion caused by the unclear description, we have revised the related contents. As you mentioned, we also think that HCHO is produced by isoprene, and isoprene is the precursor of HCHO. Meanwhile, Section 3.3.1 of HCHO in situ formation pathways also showed that isoprene is the precursor of HCHO. The revised contents in the manuscript were as follows:

“Factor 4 was characterized by a high percentage of isoprene, and the isoprene is an important precursor of HCHO (detailed discussion in Section 3.3.1). Thus, Factor 4 was designated as biogenic source, which produced HCHO from isoprene by photochemical process (Sindelarova et al., 2022; Na et al., 2004).”

3. What is the real meaning of “secondary formation”? Again, it seems likely that the HCHO from those other sources is a mix of primary and secondary. It seems more accurate to call it “Ozone associated HCHO.” This is a general shortcoming of using

PMF to parse something like HCHO and it should be acknowledged and clarified.

**Response:** We strongly agree with you that photochemical processes could lead to the deviation between the primary and secondary sources of HCHO by the PMF model. Thus, apportioning HCHO sources using the PMF model should be approached with care. The relationships between the factor contributions to each species and  $K_{OH}$  value for species in Figure 5 conform to these distribution characteristics, confirming the reasonable PMF results identified as the sources of HCHO. In our study,  $O_3$  is used as a surrogate for photochemical processes to determine the secondary fraction of HCHO. Therefore, we think it is more appropriate to interpret this as follows:

“Factor 1 was characterized by a high load of  $O_3$ , attributed to the intensive photochemical processes, that is, secondary formation of HCHO (Zeng et al., 2019; Ling et al., 2017; Li et al., 2010). Meanwhile, secondary HCHO measured at the study site includes in-situ photochemical production and regional transport.”

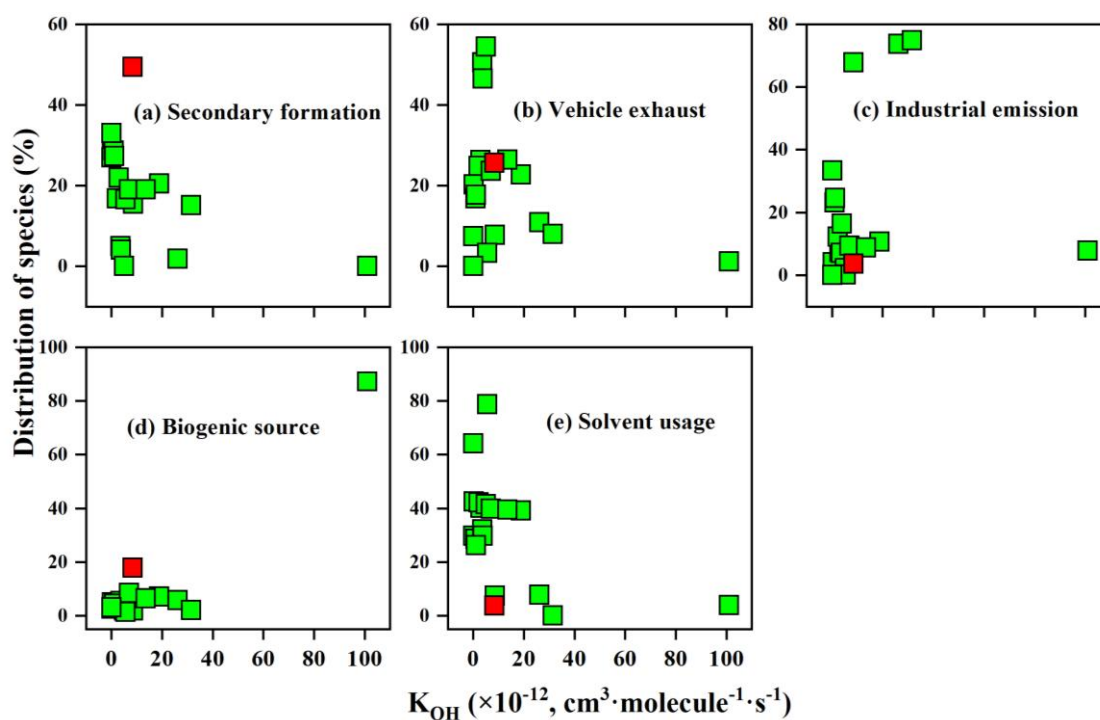


**Figure 5. Relationship between the factor contributions to each species and  $K_{OH}$  values (representing chemical activities) of the species. Each square represents one species, while HCHO is represented as a square in red.**

Data and Code Availability: According to FAIR standards, the observations and box model code should be publicly available without having to request them from the author.

**Response:** Observations results are provided in the manuscript, and the box model code is publicly available on the website of <http://mcm.leeds.ac.uk/MCM/>.

### Specific Comments

L24: The method for determining HCHO contributions should be stated here.

**Response:** Thanks for your suggestion, we have added the method, and the revised sentence in the manuscript is as follows:

“Positive Matrix Factorization (PMF) model results showed that secondary formation made the largest contributions to HCHO (49% in spring and 46% in autumn), followed by vehicle exhaust (25% and 20%) and biogenic emission (18% and 24%) in this study.”

L59 – 62: suggest deletion of this sentence.

**Response:** Thanks for your suggestion, we have deleted the sentence.

146: why is the error factor 10% instead of actual measurement accuracy?

**Response:** We are sorry for the unclear introduction, and the error factor depends on actual measurement accuracy. Because the measurement accuracies for all the species were <10%, the uncertainty of the concentrations input into the model was set as 10% based on experience. We have corrected the description as follows:

“*EF* (error factor) is set as 10% because of the <10% measurement accuracies for all the species (Ling et al., 2016; Zeng et al., 2019).”

L166: How is the boundary layer height determined?

**Response:** We have done sensitivity tests of the boundary layer height, and the sensitivity model running with different maximum mixing heights (1000 and 2000 m) indicated that its impacts on the modeling results (e.g. simulated HO<sub>x</sub> concentrations and OH production rate) were negligible. Hence, we determined the mixing layer height was assumed to vary from 300 m at night to 1500 m in the afternoon, and this parameter has been widely adopted in previous studies (Chen et al., 2020; Liu et al., 2022).

L173: updating constraints at hourly intervals is too coarse and likely leads to model artifacts due to step changes in photolysis and other parameters. 10–15 minute time steps are more appropriate for science-grade simulations.

**Response:** We strongly agree with your suggestions of science-grade simulations of 10–15 minute time steps. We considered the 10-minute and 1-hour time steps, and compared the simulated and observed HCHO in the two simulation scenarios (Fig R2). In general, both the two simulation scenarios overestimated HCHO concentration, while the overestimation of the simulated HCHO value in 10-minute scenario is significantly higher than that in 1-hour scenario. As we described in our introduction section, Xiamen frequently appeared O<sub>3</sub> pollution events in spring and autumn, because the meteorological conditions were governed by weather systems such as the quasi-

stationary front and the west pacific subtropical high, which enhanced the formation and accumulation of photochemical pollutants. Hence, the air mass in spring and autumn is not stable. Even if we try to choose relatively stagnant weather in spring and autumn in our study, the influence of meteorology still cannot be ignored. Since the model is a 0-dimensional model lacking regional transport, the simulated results will be overestimated to a certain extent. HCHO is a reactive carbonyl compound in the troposphere, if the model constraint becomes 10 minutes, the precursors are effectively replenished, leading to the accelerated production rates of HCHO and accumulated HCHO concentrations, which will naturally amplify the impacts of regional transport. Meanwhile, the primary HCHO emissions also affect the discrepancy between simulated and observed results. As I mentioned in the second question, the IOAs in 1-hour scenario are 0.83 in spring and 0.80 in autumn, which were in the reasonable IOA ranges from 0.68 to 0.89, while the IOAs in 10-minute scenario are 0.45 in spring and 0.43 in autumn. Hence, the 1 hour time step in this research was more reasonably acceptable and suitable. In related previous studies, the time step of 1 hour was widely adopted to study HCHO mechanism based on OBM (Zhang et al., 2021; Yang et al., 2020; Zeng et al., 2019).

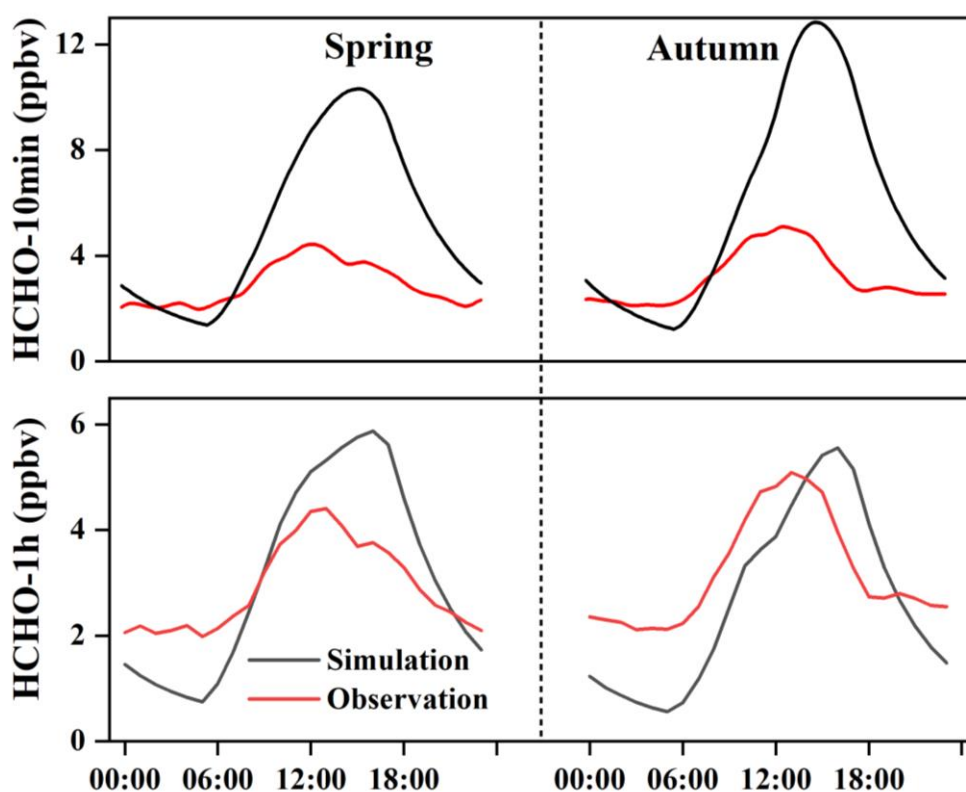


**Figure R2. The simulated and observed HCHO of 10-minute and 1-hour time steps.**

Figure 2: There is little utility in showing atmospheric pressure and all 3 J's. You could remove the bottom panels and replace pressure in the top panels with shaded J(NO<sub>2</sub>).

**Response:** Thanks for your suggestion. We have changed Figure 2 accordingly, and the revised figures were shown below:

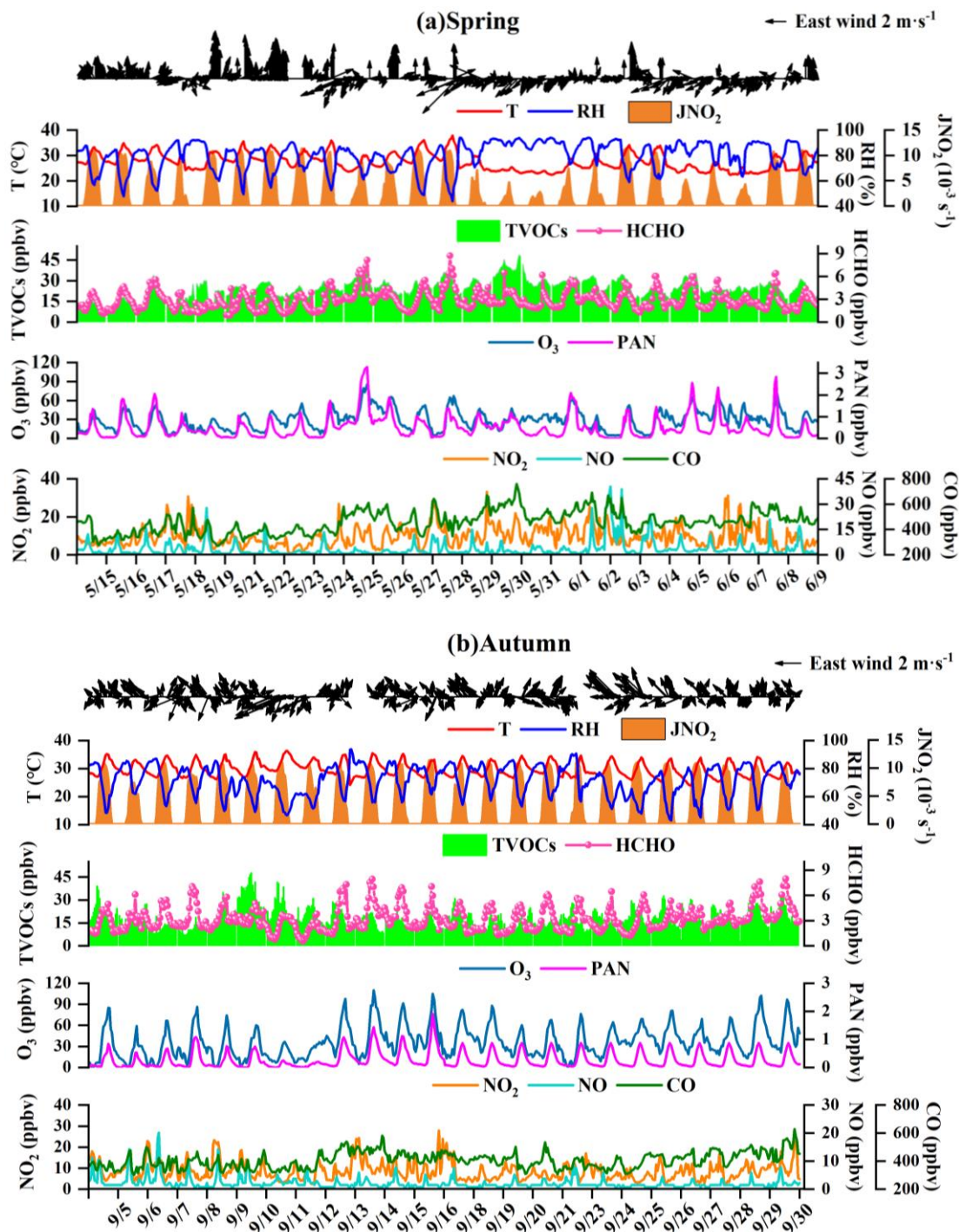


**Figure 2. Time series of HCHO, air pollutants, and meteorological parameters photolysis rate constants in (a) spring and (b) autumn.**

L174: JNO<sub>2</sub> is strongest in the visible, so applying a scaling factor from this variable alone may not capture variations in the UV (e.g. due to aerosol). How well does this JNO<sub>2</sub> parameterization predict other measured J's, like JO<sup>1</sup>D or JHCHO?

**Response:** Thanks for your suggestion. Our previous study showed that particulate pollution was slight in Xiamen, which could affect solar radiation by the light-absorbing component, and the concentrations of particulate matter had not exceeded the National Ambient Air Quality Standard (Class II: 75 μgm<sup>-3</sup>) for a whole year (Hu et al., 2022; Deng et al., 2020). Therefore, UV and JNO<sub>2</sub> showed a good correlation in our research (R<sup>2</sup>=0.97). Figure R3 shows the Scatter plots of JNO<sub>2</sub> versus UV in our study.

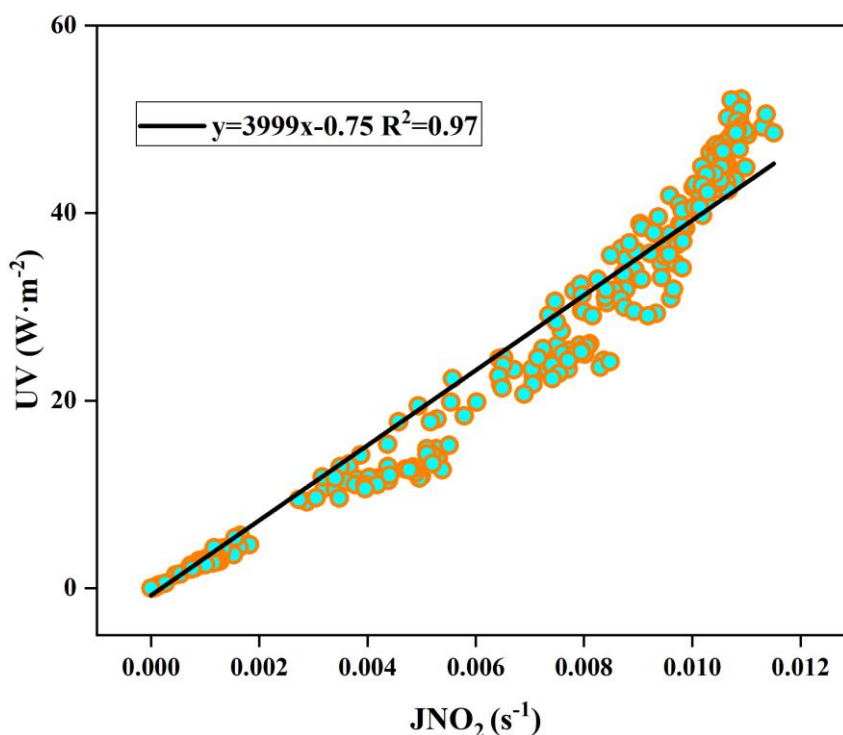


**Figure R3. The Scatter plots of JNO<sub>2</sub> versus UV at our study site.**

Photolysis frequencies of other species were calculated in the model using the following function of solar zenith angle ( $\gamma$ ) and scaled to the ratio of measured to calculated jNO<sub>2</sub> to represent the effect from clouds:

$$J = l \times (\cos\gamma)^m \times e^{-n \times \sec\gamma}$$

Where, the optimal values of parameters l, m, and n for each photolysis frequency were adopted (Saunders et al., 2003). And Figure R4 shows the calculated and observed JO<sup>1</sup>D and JHCHO in our study, and the results showed that the JNO<sub>2</sub> parameterization predicts JO<sup>1</sup>D and JHCHO resulting in uncertainty of ~20%, which is within the allowable error range. In our study, the important photolysis rate constants of JHCHO, JO<sup>1</sup>D, JNO<sub>2</sub>, JH<sub>2</sub>O<sub>2</sub>, JHONO, and JNO<sub>3</sub> were all monitored by a photolysis spectrometer (PFS-100, Focused Photonics Inc., Hangzhou, China), which furtherly guaranteed the reliability of the model simulation.

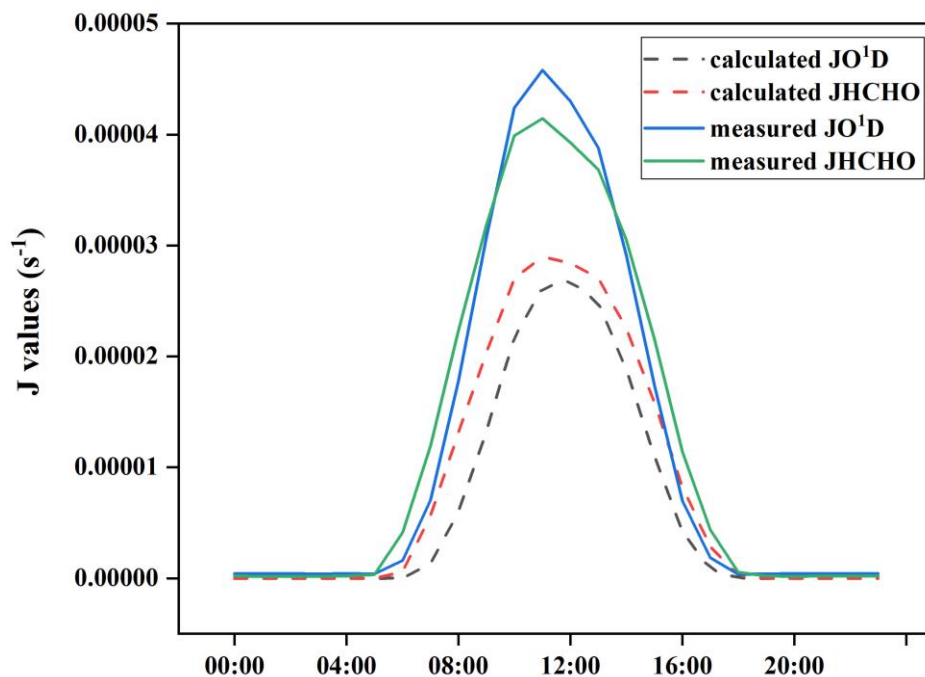


**Figure R4. The calculated and observed JO<sup>1</sup>D and JHCHO in our study**

L182: Why 20%? Are RIR values sensitive to this choice? Why not a smaller value (like 1%) so that radical resulting perturbations are locally linear?

**Response:** In the process of reduction effect, to avoid the possible numerical calculation errors and minimize the interference to the model system, in the model test phase, a series of trial calculations were performed on the value of source reduction ( $\Delta X/X=5\%$ , 10%, 20%, 30%, 40%), it is found that the error and interference of the model are smaller when  $\Delta X/X=20\%$ . Hence, we choose to reduce it by 20% for research, and most of the previous related research also chose 20% to analyze sensitivity with less error (Yang et al., 2020; Liu et al., 2021; Chen et al., 2020; Wang et al., 2020). We have revised the sentence in the manuscript as follows:

“The  $\Delta X/X$  represents the reduction ratio of each targeted HCHO precursor group, and the value adopted is 20%, which is of benefit to avoiding possible numerical calculation errors and minimizing the interference to the model system.”

L222: What other data supports “replenishment of HCHO primary emissions and accumulation of pollutants”?

**Response:** Thanks for your suggestion. The conditional probability function (CPF) is used to show the wind directions that dominate a high concentration of a pollutant and the probability, which is therefore potentially very useful for source identification and characterization (Zhang et al., 2021; Uria-Tellaetxe and Carslaw, 2014). Figure S3 shows CPF polar plots during daytime (06:00-17:00 LT) and the nighttime. These plots

showed that the clearest areas where the probabilities were higher were to the northwest and southeast from continental air masses with relatively high wind speed ( $>3 \text{ m}\cdot\text{s}^{-1}$ ) during the daytime. High HCHO values during the nighttime easily happened in the wind direction of the southeast with low wind speed ( $<2 \text{ m}\cdot\text{s}^{-1}$ ), showing the influence of urban plumes with intensive vehicle emissions from the downtown of Xiamen. The plots clearly revealed potential sources of HCHO. The HCHO during the daytime was affected by regional transport and local emission, and the HCHO at night mainly from replenishment of local HCHO primary emissions and accumulation of pollutants. We have added a CPF analysis in the manuscript and the Supplementary.

“The conditional probability functions (CPF) polar plots (Fig. S3) clearly revealed the relationship between high HCHO concentrations and wind (Zhang et al., 2021a; Uria-Tellaetxe and Carslaw, 2014). The results suggest that high HCHO values during the nighttime easily happened in the wind direction of the southeast with low wind speed ( $<2 \text{ m}\cdot\text{s}^{-1}$ ), showing the influence of urban plumes with intensive vehicle emissions from the downtown of Xiamen. Hence, the high HCHO levels during the nighttime were mostly formed locally, such as the replenishment of HCHO primary emissions and accumulation of pollutants under stable weather conditions.”

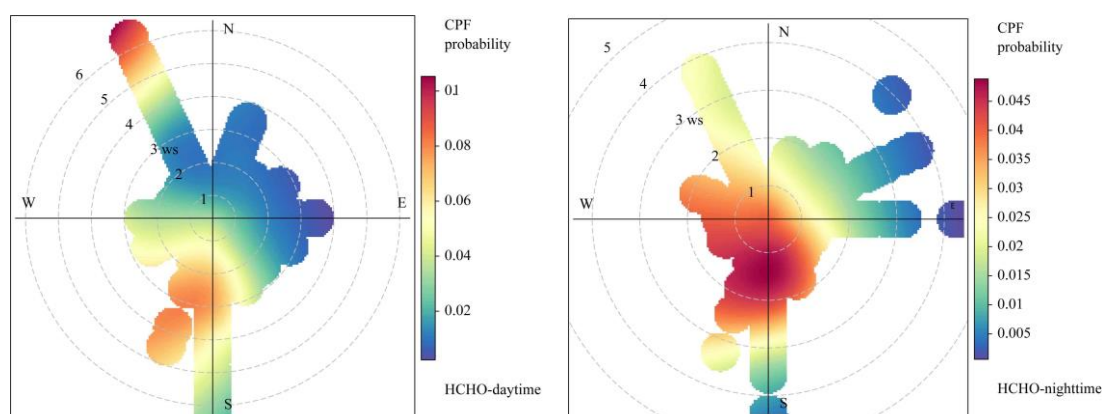


**Figure S3. The CPF polar plots during daytime (06:00-17:00 LT) and the nighttime.**

L291: “under the intense solar radiation” is vague. Be quantitative. Based on Fig. 3, the J values are higher by 20% in autumn.

**Response:** Thanks for your suggestion, we have added the calculated quantization results accordingly.

L29: The net production rate seems at odds with diurnal cycle of  $d\text{HCHO}/dt$ . At times, the observations show increasing HCHO when the model predicts loss, and vice versa. This is consistent with my second general comment about the model being over-constrained.

**Response:** The discrepancy between the simulated and observed HCHO net production

rate is inevitable. This could be partially attributed to the limitation of the OBM model, which only considers the photochemical reactions, dry deposition, and dilution mixing within the boundary layer, while the primary emissions of HCHO and the transport of air masses are not considered. Although some bias exists, the model results still provide valuable information on secondary formation of HCHO in our study based on the model validation of IOA (0.83 in spring and 0.80 in autumn in our research). The detailed reasons for the discrepancy between the simulated and observed HCHO are also described in our manuscript.

L301: CH<sub>3</sub>O<sub>2</sub> comes from many precursors, so it is not quite fair to distinguish this from other RO<sub>2</sub> precursors. This should be somehow stated or made clear, that the “RO + O<sub>2</sub>” bars in Fig. 5 are lower limits.

**Response:** Thanks for your suggestion, we have stated the pathway of CH<sub>3</sub>O+O<sub>2</sub> in the manuscript, as follows:

“CH<sub>3</sub>O radicals were from aromatics, alkenes, and isoprene, therefore, we provided a lower limit of the other pathways of RO+O<sub>2</sub> in this study (Zhang et al., 2021a; Li et al., 2014; Yang et al., 2020; Zhu et al., 2020).”

L312: “significantly higher” is not quantitative. Also, the loss rate might be higher because HCHO is higher. What is the difference in HCHO lifetimes between the two periods?

**Response:** Thanks for your suggestion, we have quantified this result, as follows. The lifetimes of HCHO in spring were around 1.21 times longer than those in autumn.

“It was worth noting that the contributions of HCHO production pathways had minor seasonal variations, while the contributions of HCHO loss pathways in autumn were 1.31 times higher than those in spring.”

Sect. 3.4.1: This section does not describe the impacts of HCHO on atmospheric oxidation.

**Response:** Atmospheric oxidation (hence atmospheric oxidation capacity-AOC) is generally defined as the sum of oxidation rates of various primary pollutants (i.e., CO, VOCs) by the oxidants (i.e., OH, O<sub>3</sub>, and NO<sub>3</sub> radicals) (Elshorbany et al., 2009; Xue et al., 2016). The hydroxyl radical (OH) is the central player in atmospheric chemistry, accounting for the majority (97%) of AOC during the daytime in our study. The OH reactivity has been widely used as an indicator of the intensity of atmospheric oxidation (Mao et al., 2010; Xue et al., 2016). Hence, the discussion of the impacts of HCHO on OH reactivity is about the impacts of HCHO on atmospheric oxidation. To avoid misunderstanding, the relevant contents were also supplemented and revised.

L421: Autumn OH is higher than any previous observations in China, at least among those cited. It is not fair to say the simulated HOx is “comparable.” This is a lot of OH. Can any model comparisons be done to observations to substantiate it?

**Response:** The observed OH values were classified into three categories: urban, remote, and forested areas (Fig. R5) (Lu et al., 2010). The observed OH daily maximum concentrations in different categories are all in the range of  $10^6$ – $10^7$  molecule·cm<sup>-3</sup>. The observations in urban areas showed a tendency for higher OH daily maximum concentrations, probably caused by the faster radical propagation from HO<sub>2</sub> with the presence of the higher NO concentrations and the presence of higher O<sub>3</sub> and OVOC concentrations. The maximum daily values of OH were observed with  $1.7 \times 10^7$  molecule cm<sup>-3</sup> in the North China Plain (Lu et al., 2012; Tan et al., 2017),  $1.2 \times 10^7$  molecule·cm<sup>-3</sup> in Chengdu (Zhang et al., 2022), and  $1.5 \times 10^7$  molecule·cm<sup>-3</sup> in PRD (Lu et al., 2019).

To verify the performance of the OBM model, regional daytime mixing ratios of OH was also estimated by a parameterization method using measured NO<sub>2</sub> and HONO concentrations and the photolysis rate constants of NO<sub>2</sub>, O<sub>3</sub>, and HONO (Wen et al., 2019; Hu et al., 2022), which fully considers the influence of photolysis and precursors on the concentration of [OH]. Figure S6 shows the OH concentrations of parameter calculation and model simulation. The calculated average regional concentrations of OH ( $9.14 \times 10^6$  molecule·cm<sup>-3</sup> in spring and  $1.24 \times 10^7$  molecule·cm<sup>-3</sup>) were very close to the OBM-simulated result ( $7.30 \times 10^6$  molecule·cm<sup>-3</sup> in spring and  $1.12 \times 10^7$  molecule·cm<sup>-3</sup>), suggesting that the OBM simulated radical concentration is reliable. The revised contents in the manuscript were as follows:

“In previous studies, the observed OH daily maximum concentrations in three areas categories (urban, remote, and forest) were all in the range of  $10^6$ – $10^7$  molecule·cm<sup>-3</sup> (Lu et al., 2010). The maximum daily values of OH were observed with  $1.7 \times 10^7$  molecule·cm<sup>-3</sup> in the North China Plain (Lu et al., 2012; Tan et al., 2017),  $1.2 \times 10^7$  molecule·cm<sup>-3</sup> in Chengdu (Zhang et al., 2022), and  $1.5 \times 10^7$  molecule·cm<sup>-3</sup> in PRD (Lu et al., 2019). We calculated OH concentrations based on measured NO<sub>2</sub> and HONO concentrations and the photolysis rate constants of NO<sub>2</sub>, O<sub>3</sub>, and HONO (Wen et al., 2019; Hu et al., 2022). The calculated average regional concentrations of OH in Fig. S6 ( $9.1 \times 10^6$  molecule·cm<sup>-3</sup> in spring and  $1.2 \times 10^7$  molecule·cm<sup>-3</sup>) were very close to the OBM-simulated result ( $7.3 \times 10^6$  molecule·cm<sup>-3</sup> in spring and  $1.1 \times 10^7$  molecule·cm<sup>-3</sup>), suggesting that the OBM simulated radical concentration is reliable.”

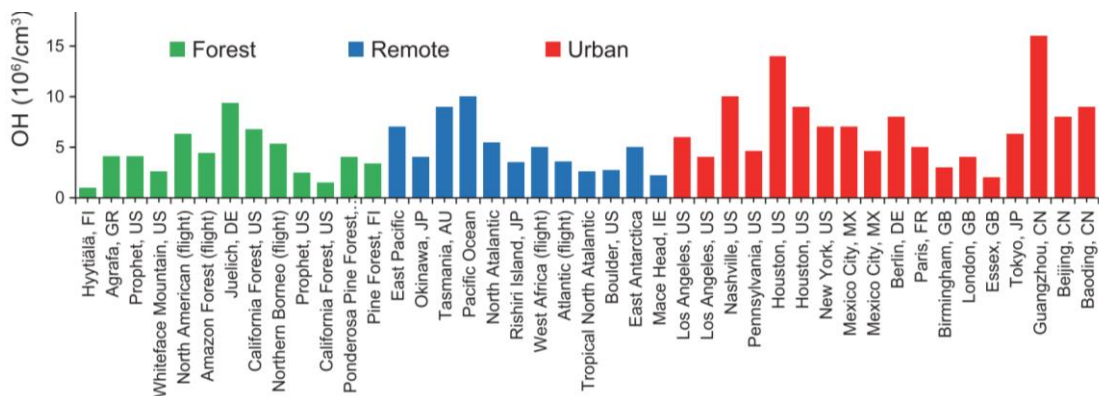


**Figure R5.** Typical observed daily averaged maximum OH concentrations at distinct different geophysical regions (i.e. urban, remote, forest areas).

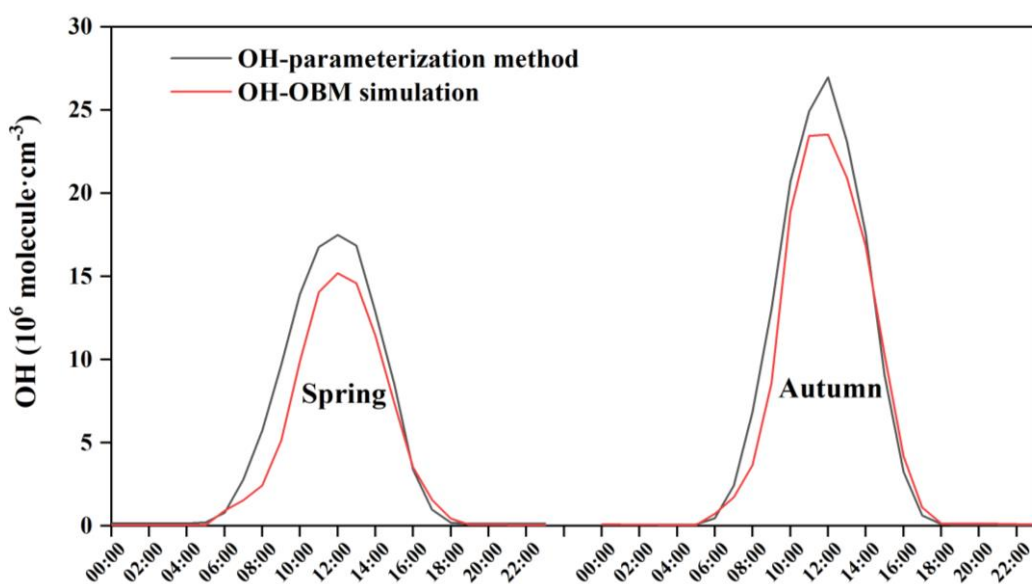


**Figure S6.** The OH concentrations of parameter calculation and model simulation.

L430: Here, and elsewhere throughout the paper (L454, L501), are long lists of numbers that don't convey anything meaningful to the reader.

**Response:** Thanks for your suggestions. We have condensed the relevant content.

Figure 9: Figure S4 is potentially a more useful figure.

**Response:** Figure S4 has been added to the manuscript of Figure 11.

L449: If the model were truly constrained to ozone, there would be no decrease in ozone photolysis between these two runs. As alluded to in the General Comments, this is potentially an artifact of hourly time steps.

**Response:** We agree with you that this is an artifact of hourly time steps. O<sub>3</sub> with a time resolution of 1 h was constrained in the model, but the O<sub>3</sub> in the model kept participating in the reaction of MCM, which was a dynamic equilibrium process. Hence, the observed O<sub>3</sub> constrains the model within the range of actual observations. Only if a species does not participate in any chemical reaction, do the observed concentrations and output concentrations in the model of this species keep the same. The loss pathways of HCHO, mainly including HCHO photolysis and its oxidation with OH radical producing HO<sub>2</sub> radical, detailed information in Section 3.3.1, played the key role in the most significant impacts of HCHO on atmospheric photochemistry. HCHO photolysis could directly produce HO<sub>2</sub> radical, which indirectly influences O<sub>3</sub> by radical chemistry. Disabling the HCHO loss pathways in the model decreased O<sub>3</sub> concentrations in the model, thus decreasing the rates of O<sub>3</sub> photolysis. In your question of L173, as mentioned before, we had explained the reasons that the 1-hour time step in this research was more reasonably acceptable and suitable than the 10 min time step.

### Technical Comments

English throughout would benefit from substantial copyediting.

**Response:** We appreciate the reviewer for the helpful suggestions. In the revised manuscript, we have addressed the comments carefully. The manuscript has been significantly revised and improved based on these suggestions.

Acronyms should only be defined after their first use.

**Response:** Thanks for your suggestions. We have checked and revised the relevant content of acronyms.

Throughout the text, numbers are reported with too many significant figures. For example, 2.94 +/- 1.28 ppbv should be 2.9 +/- 1.3 ppbv. Also, it is often unclear what the averages and uncertainties/variabilities refer to (averaged of what period, at what time resolution).

**Response:** Thanks for your suggestions. The time resolution of averages and uncertainties/variabilities in our study refer to 1 hour, and the periods of averages are also added. We have revised the relevant expression in the manuscript.

### Reference:

Chen, T., Xue, L., Zheng, P., Zhang, Y., Liu, Y., Sun, J., Han, G., Li, H., Zhang, X., Li, Y., Li, H., Dong, C., Xu, F., Zhang, Q., and Wang, W.: Volatile organic compounds and ozone air pollution in an oil production region in northern China, *Atmospheric Chemistry and Physics*, 20, 7069-7086, 10.5194/acp-20-7069-2020, 2020.

Chen, W. T., Shao, M., Lu, S. H., Wang, M., Zeng, L. M., Yuan, B., and Liu, Y.:

Understanding primary and secondary sources of ambient carbonyl compounds in Beijing using the PMF model, *Atmospheric Chemistry and Physics*, 14, 3047-3062, 10.5194/acp-14-3047-2014, 2014.

Cheng, Y., Lee, S.C., Huang, Y., Ho, K.F., Ho, S.S.H., Yau, P.S., Louie, P.K.K., Zhang, R.J., 2014. Diurnal and seasonal trends of carbonyl compounds in roadside, urban, and suburban environment of Hong Kong. *Atmos. Environ.* 89, 43–51.

Deng, J., Guo, H., Zhang, H., Zhu, J., Wang, X., and Fu, P.: Source apportionment of black carbon aerosols from light absorption observation and source-oriented modeling: an implication in a coastal city in China, *Atmos. Chem. Phys.*, 20, 14419–14435, <https://doi.org/10.5194/acp-20-14419-2020>, 2020.

Guo, H., 2009. Concurrent observations of air pollutants at two sites in the Pearl River Delta and the implication of regional transport. *Atmos. Chem. Phys.* 9, 7343–7360.

Guo, H., Ling, Z. H., Cheung, K., Wang, D. W., Simpson, I. J., and Blake, D. R.: Acetone in the atmosphere of Hong Kong: Abundance, sources and photochemical precursors, *Atmospheric Environment*, 65, 80-88, 10.1016/j.atmosenv.2012.10.027, 2013.

Hu, B., Duan, J., Hong, Y., Xu, L., Li, M., Bian, Y., Qin, M., Fang, W., Xie, P., and Chen, J.: Exploration of the atmospheric chemistry of nitrous acid in a coastal city of southeastern China: results from measurements across four seasons, *Atmos. Chem. Phys.*, 22, 371–393, <https://doi.org/10.5194/acp-22-371-2022>, 2022.

Jiang, Y., Xue, L., Gu, R., Jia, M., Zhang, Y., Wen, L., Zheng, P., Chen, T., Li, H., Shan, Y., Zhao, Y., Guo, Z., Bi, Y., Liu, H., Ding, A., Zhang, Q., and Wang, W.: Sources of nitrous acid (HONO) in the upper boundary layer and lower free troposphere of the North China Plain: insights from the Mount Tai Observatory, *Atmospheric Chemistry and Physics*, 20, 12115-12131, 10.5194/acp-20-12115-2020, 2020.

Li, X., Rohrer, F., Brauers, T., Hofzumahaus, A., Lu, K., Shao, M., Zhang, Y. H., and Wahner, A.: Modeling of HCHO and CHOCHO at a semi-rural site in southern China during the PRIDE-PRD2006 campaign, *Atmospheric Chemistry and Physics*, 14, 12291-12305, 10.5194/acp-14-12291-2014, 2014.

Li, Y., Shao, M., Lu, S., Chang, C.-C., Dasgupta, P.K., 2010. Variations and sources of ambient formaldehyde for the 2008 Beijing Olympic games. *Atmos. Environ.* 44, 2632–2639.

Ling, Z. H., Zhao, J., Fan, S. J., and Wang, X. M.: Sources of formaldehyde and their contributions to photochemical O<sub>3</sub> formation at an urban site in the Pearl River Delta, southern China, *Chemosphere*, 168, 1293-1301, 10.1016/j.chemosphere.2016.11.140, 2017.

Ling, Z.H., Guo, H., Simpson, I.J., Saunders, S.M., Lam, S.H.M., Lyu, X.P., et al., 2016. New insight into the spatiotemporal variability and source apportionments of C<sub>1</sub>–C<sub>4</sub> alkyl nitrates in Hong Kong. *Atmos. Chem. Phys.* 16, 8141–8156.

Liu, T., Hong, Y., Li, M., Xu, L., Chen, J., Bian, Y., Yang, C., Dan, Y., Zhang, Y., Xue, L., Zhao, M., Huang, Z., and Wang, H.: Atmospheric oxidation capacity and ozone pollution mechanism in a coastal city of southeastern China: analysis of a typical photochemical episode by an observation-based model, *Atmospheric Chemistry and Physics*, 22, 2173-2190, 10.5194/acp-22-2173-2022, 2022.

Liu, Y., Shen, H., Mu, J., Li, H., Chen, T., Yang, J., Jiang, Y., Zhu, Y., Meng, H., Dong, C., Wang, W., and Xue, L.: Formation of peroxyacetyl nitrate (PAN) and its impact on ozone production in the coastal atmosphere of Qingdao, North China, *Sci Total Environ*, 778, 146265, 10.1016/j.scitotenv.2021.146265, 2021.

Liu, Y., Yuan, B., Li, X., Shao, M., Lu, S., Li, Y., Chang, C.C., Wang, Z., Hu, W., Huang, X., He, L., Zeng, L., Hu, M., Zhu, T., 2015. Impact of pollution controls in Beijing on atmospheric oxygenated volatile organic compounds (OVOCs) during the 2008 Olympic Games: observation and modeling implications. *Atmos. Chem. Phys.* 15, 3045–3062.

Louie, P.K.K., Ho, J.W.K., Tsang, R.C.W., Blake, D.R., Lau, A.K.H., Yu, J.Z., Yuan, Z., Wang, X., Shao, M., Zhong, L., 2013. VOCs and OVOCs distribution and control policy implications in Pearl River Delta region. *China. Atmos. Environ.* 76, 125–135.

Lu K, Guo S, Tan Z, Wang H, Shang D, Liu Y, Li X, Wu Z, Hu M, Zhang Y: Exploring atmospheric free-radical chemistry in China: the self-cleansing capacity and the formation of secondary air pollution. *National Science Review*, 6(3):579-594, 2019.

Lu KD and Zhang YH. Observations of HO(x) Radical in field studies and the analysis of its chemical mechanism. *Prog Chem* 2010; 22: 500–14.

Saunders, S. M., Jenkin, M. E., Derwent, R. G., and Pilling, M.J.: Protocol for the development of the Master Chemical Mechanism, MCM v3 (Part A): tropospheric degradation of nonaromatic volatile organic compounds, *Atmos. Chem. Phys.*, 3, 161–180, <https://doi.org/10.5194/acp-3-161-2003>, 2003.

Tan, Z., Lu, K., Jiang, M., Su, R., Wang, H., Lou, S., Fu, Q., Zhai, C., Tan, Q., Yue, D., Chen, D., Wang, Z., Xie, S., Zeng, L., and Zhang, Y.: Daytime atmospheric oxidation capacity in four Chinese megacities during the photochemically polluted season: a case study based on box model simulation, *Atmospheric Chemistry and Physics*, 19, 3493-3513, 10.5194/acp-19-3493-2019, 2019.

Uria-Tellaetxe, I., and Carslaw, D. C.: Conditional bivariate probability function for source identification, *Environ. Model. Softw.*, 59, 1-9, 2014.

Wang, H., Lyu, X., Guo, H., Wang, Y., Zou, S., Ling, Z., Wang, X., Jiang, F., Zeren, Y., Pan, W., Huang, X., and Shen, J.: Ozone pollution around a coastal region of South China Sea: interaction between marine and continental air, *Atmos. Chem. Phys.*, 18, 4277–4295, 10.5194/acp-18-4277-2018, 2018.

Wang, M., Chen, W., Zhang, L., Qin, W., Zhang, Y., Zhang, X., and Xie, X.: Ozone

pollution characteristics and sensitivity analysis using an observation-based model in Nanjing, Yangtze River Delta Region of China, *J Environ Sci (China)*, 93, 13-22, 10.1016/j.jes.2020.02.027, 2020.

Wang, Q., Chen, W., Xu, W.T., Yang, P., Liu, Y.Y., Ma, J.Y., Hua, D.Z.: Formaldehyde Reaction Cell, CN212207248U, <https://kns.cnki.net/kcms/detail/detail.aspx?FileName=CN212207248U&DbName=SCPD2020>, 2020.

Wen, L., Chen, T., Zheng, P., Wu, L., Wang, X., Mellouki, A., Xue, L., and Wang, W.: Nitrous acid in marine boundary layer over eastern Bohai Sea, China: Characteristics, sources, and implications, *Sci. Total Environ.*, 670, 282–291, <https://doi.org/10.1016/j.scitotenv.2019.03.225>, 2019.

Yang, X., Xue, L., Wang, T., Wang, X., Gao, J., Lee, S., Blake, D.R., Chai, F., Wang, W., 2018. Observations and explicit modeling of summertime carbonyl formation in Beijing: identification of key precursor species and their impact on atmospheric oxidation chemistry: observations and explicit modeling of summertime carbonyl formation in Beijing: *Int. J. Geophys. Res. Atmos.* 123.

Yang, X., Xue, L., Yao, L., Li, Q., Wen, L., Zhu, Y., Chen, T., Wang, X., Yang, L., Wang, T., Lee, S., Chen, J., Wang, W., 2017. Carbonyl compounds at Mount Tai in the North China Plain: characteristics, sources, and effects on ozone formation. *Atmos. Res.* 196, 53–61.

Yang, X., Zhang, G., Sun, Y., Zhu, L., Wei, X., Li, Z., and Zhong, X.: Explicit modeling of background HCHO formation in southern China, *Atmospheric Research*, 240, 104941, 10.1016/j.atmosres.2020.104941, 2020.

Yang, Z., Cheng, H.R., Wang, Z.W., Peng, J., Zhu, J.X., Lyu, X.P., Guo, H., 2019. Chemical characteristics of atmospheric carbonyl compounds and source identification of formaldehyde in Wuhan. Central China. *Atmos Res.* 228, 95–106.

Yuan, B., Shao, M., de Gouw, J., Parrish, D. D., Lu, S., Wang, M., Zeng, L., Zhang, Q., Song, Y., Zhang, J., and Hu, M.: Volatile organic compounds (VOCs) in urban air: How chemistry affects the interpretation of positive matrix factorization (PMF) analysis, *Journal of Geophysical Research: Atmospheres*, 117, n/a-n/a, 10.1029/2012jd018236, 2012.

Zeng, P., Lyu, X., Guo, H., Cheng, H., Wang, Z., Liu, X., and Zhang, W.: Spatial variation of sources and photochemistry of formaldehyde in Wuhan, Central China, *Atmospheric Environment*, 214, 116826, 10.1016/j.atmosenv.2019.116826, 2019.

Zhang, G., Hu, R., Xie, P., Lu, K., Lou, S., Liu, X., Li, X., Wang, F., Wang, Y., Yang, X., Cai, H., Wang, Y., and Liu, W.: Intercomparison of OH radical measurement in a complex atmosphere in Chengdu, China, *Sci Total Environ*, 838, 155924, 10.1016/j.scitotenv.2022.155924, 2022.

Zhang, K., Duan, Y., Huo, J., Huang, L., Wang, Y., Fu, Q., Wang, Y., and Li, L.: Formation mechanism of HCHO pollution in the suburban Yangtze River Delta region,

China: A box model study and policy implementations, *Atmospheric Environment*, 267, 118755, 10.1016/j.atmosenv.2021.118755, 2021a.

Zhang, K., Huang, L., Li, Q., Huo, J., Duan, Y., Wang, Y., Yaluk, E., Wang, Y., Fu, Q., and Li, L.: Explicit modeling of isoprene chemical processing in polluted air masses in suburban areas of the Yangtze River Delta region: radical cycling and formation of ozone and formaldehyde, *Atmospheric Chemistry and Physics*, 21, 5905-5917, 10.5194/acp-21-5905-2021, 2021b.